

PROCEEDINGS OF SPIE

[SPIDigitalLibrary.org/conference-proceedings-of-spie](https://spiedigitallibrary.org/conference-proceedings-of-spie)

Multi-object spectroscopy on the Hobby-Eberly Telescope low-resolution spectrograph

Wolf, Marsha, Hill, Gary, Mitsch, Wolfgang, Hessman, Frederic, Altmann, Werner, et al.

Marsha J. Wolf, Gary J. Hill, Wolfgang Mitsch, Frederic V. Hessman, Werner Altmann, Keith L. Thompson, "Multi-object spectroscopy on the Hobby-Eberly Telescope low-resolution spectrograph," Proc. SPIE 4008, Optical and IR Telescope Instrumentation and Detectors, (16 August 2000); doi: 10.1117/12.395476

SPIE.

Event: Astronomical Telescopes and Instrumentation, 2000, Munich, Germany

Multiobject spectroscopy on the Hobby-Eberly Telescope Low Resolution Spectrograph

Marsha J. Wolf^{*a}, Gary J. Hill^a, Wolfgang Mitsch^b, Frederic V. Hessman^c, Werner Altmann^d,
Keith L. Thompson^e

^aMcDonald Observatory/Astronomy Department, University of Texas at Austin, Austin, TX 78712,
USA

^bUniversitäts-Sternwarte, Ludwig-Maximilians-Universität, Scheinerstr. 1, D-81679 München,
Germany

^cUniversitäts-Sternwarte, Georg-August-Universität, Geismarlandstr. 11, D-37083 Göttingen, Germany

^dKonstruktionsbüro Werner Altmann, Sonnenstr. 41, Haselbach, 94113 Tiefenbach, Germany

^ePhysics Department, Stanford University, 382 Via Pueblo Mall, Stanford, CA 94305-4060, USA

ABSTRACT

The Low Resolution Spectrograph (LRS) is the first facility instrument on the 9.2 m Hobby-Eberly Telescope (HET). The LRS has three operational modes: imaging, long-slit spectroscopy and multi-object spectroscopy (MOS). We present the design and early operations performance of the LRS MOS unit, which provides 13 slitlets, each 1.3 arcsec by 15 arcsec, on 19.6 arcsec centers, within the 4 arcmin (50 mm) field of view of the HET. This type of remotely configurable unit was chosen over the more conventional slit masks due to the queue scheduling of the HET, and the instrument's remote location at the prime focus of the telescope. A restricted envelope around the HET focus at the LRS port forced a very compact design. The MOS unit has miniature mechanisms based on custom cross-roller stages and 0.25 mm pitch lead-screws. Gearing stepper motors with 10 mm diameters drive the 13 axes at 0.8 micron per step. The precision of the mechanism is far greater than required by the HET plate scale of 205 microns per arcsec, but results in a robust unit. The slitlets were fabricated at the University of Texas by shadow-masking the slit area with a wire and vacuum depositing aluminum onto the silica substrates. Both sides are then coated with MgF₂, which serves as an antireflection coating and a protective layer. Web-based software is available for optimizing the orientation of the MOS unit and the placement of slitlets on objects in the field. These setups can be downloaded to the unit for configuration outside of the beam while the HET is slewing to its next target in the queue, or while the LRS is used in imaging mode for setup on faint objects. The preliminary results presented here are from one commissioning run with the MOS, where the unit appears to be meeting performance specifications.

Keywords: multiobject, spectroscopy, 8-meter class, instrumentation, HET, LRS, low-resolution

1. INTRODUCTION

1.1 The Hobby-Eberly Telescope

The HET^{1,2,3,4} (a collaboration of the University of Texas at Austin, Pennsylvania State University, Stanford, Georg-August-Universität, Göttingen, and Ludwig-Maximilians-Universität, Munich) began science operations in September 1999. It incorporates an innovative fixed elevation design that enabled the construction of an 8-meter class telescope for approximately one tenth the cost of conventional designs. It serves as the prototype for a new generation of telescopes, as the first copy is beginning construction in South Africa, the Southern Africa Large Telescope (SALT). A star tracker⁵ sits atop the telescope to move the prime focus instruments and fiber instrument feeds along the telescope's focal sphere during a science exposure. Full azimuthal movement, coupled with the restrictions in elevation, allow 70% sky coverage from

* Correspondence: Email: mwolf@astro.as.utexas.edu; Telephone: 512-471-0445; Fax: 512-471-6016

McDonald Observatory in West Texas. The pupil is 9.2 m in diameter, and sweeps over the 11-m primary mirror as the tracker follows objects for between 40 minutes (in the south at $\delta = -10.3^\circ$) and 2.8 hours (in the north at $\delta = +71.6^\circ$). The maximum track time on a single field per night is 5.6 hours and occurs at a declination of $+63^\circ$. These times are quoted for an effective 8-m aperture since the pupil partially falls off the mirror near the extremes of the tracks.

The 11-m primary mirror, shown in Figure 1, consists of 91 mirror segments, each 1-m in diameter. Segments are mounted on a steel truss that expands and contracts with ambient temperature. The initial operational model for mirror alignment was to use the center of curvature alignment sensor (CCAS) once per hour to align the primary mirror and then to predict and correct truss movements during the hour via a thermal model. This method was plagued by two major problems: the truss movements were found to be inelastic and not predictable, and the CCAS has never worked properly for fine mirror alignment. Both problems are currently being solved. Initial mirror alignment is achieved via a semi-automated stacking technique developed by the onsite staff, which currently aligns the mirrors to 0.9 arcsec.³ The CCAS, a polarization shearing interferometer, was delivered untested and many bugs are now systematically being worked out. It is expected that the instrument will be operational later this year for fine mirror alignment. The inelastic truss movement

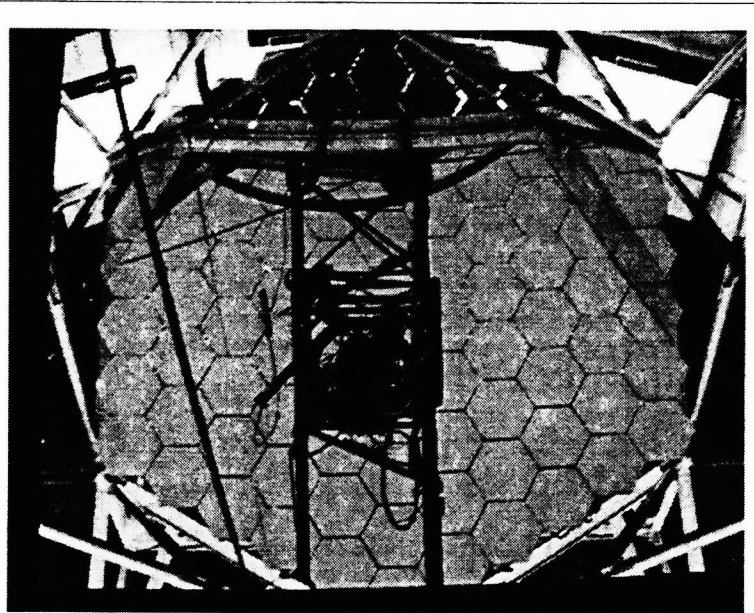


Figure 1. The HET primary mirror with a reflection of the tracker and prime focus instrument platform (PFIP) above.

problem will be solved by a segment alignment maintenance system (SAMS)⁶ that will place edge sensors on the mirror segments to provide feedback to an active control system. Once these two systems are fully operational, the HET is expected to deliver a typical image quality of 1.3 arcsec, and 1.0 arcsec under the best conditions. The slits on the LRS MOS unit were designed for this optimal operation and are 1.3 arcsec wide.

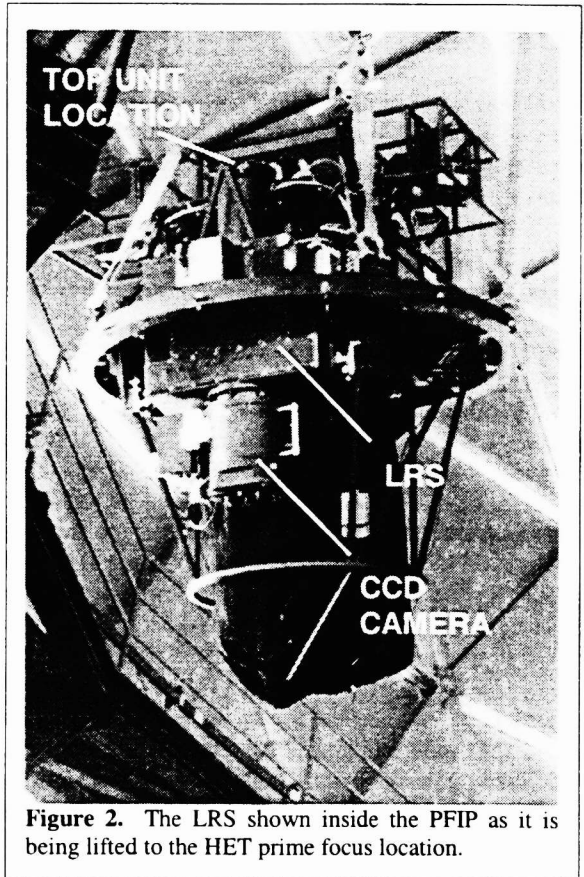


Figure 2. The LRS shown inside the PFIP as it is being lifted to the HET prime focus location.

The principal niches for the HET will be large surveys and temporal phenomena, taking advantage of the queue-scheduling of the telescope. As a result, the LRS is a very robust instrument with high throughput in order to take greatest advantage of the limited track-times on any given source. The HET sits at 35° to the zenith, so there is an approximately constant gravity loading along the axis of the LRS. The prime focus instrument platform (PFIP) can rotate about the axis of the corrector in order to access different position angles (PAs) on the sky, but during a typical track the rotation will only change by a few degrees. As a result, flexure during a track is not an issue. This situation is comparable to that for a Nasmyth mounted instrument.

1.2 The Marcario Low Resolution Spectrograph

The Marcario LRS is a grism spectrograph with three modes of operation: imaging, longslit, and multiobject. The field of view (FOV) of the HET is 4 arcmin in diameter (50 mm at $f/4.6$), and the LRS 13-slitlet MOS unit covers this field. Resolving powers between $R = \lambda/\Delta\lambda \sim 600$ and 3000 with a 1 arcsec wide slit are achieved with a variety of grisms, two of which can be carried by the instrument at any one time. The CCD is a 3072x1024 device with 15 μm pixels, and the image

scale is 0.236 arcsec per pixel. The LRS rides in the PFIP (Figure 2) on the tracker, allowing it to image as well as take spectra.

The physical constraints of the PFIP dictated that the LRS design be linear with a fold, so a refractive collimator and grism disperser were adopted. The refractive collimator of the LRS has a doublet 85.5 mm behind the slit plane and a triplet 740 mm behind the slit plane.⁷ A mirror folds the collimator to conform to the space envelope. The space between the collimator triplet and the camera is 330 mm to allow room for even the largest echelle grisms. Two grisms can be carried in the LRS at once and are inserted into the beam against hard stops by pneumatic cylinders.

The camera is an integral unit which includes the CCD head and cryocooler. The CCD system was designed by P. MacQueen.⁸ Since the camera accepts the collimated beam, making its alignment with the rest of the instrument noncritical, removing it for maintenance or swapping it for the IR camera is straight-forward. The camera is a $f/1.4$ catadioptric with all spherical surfaces.⁷ For the LRS, this design is preferred over a refractive design due to the required fast focal ratio, the ability to tolerate a central obstruction, and the relatively low cost. Analysis of the throughput of suitable (but slower) refractive designs indicated that when glass transmission and reflection losses are considered, a refractive camera would have only a minor throughput advantage, at best.

1.3 Overview of the MOS unit

The MOS unit⁹ sits in the top unit of the LRS (Figure 2). It has 13 independent slitlets moved by miniature geared stepper motors and lead screws on precision miniature cross-roller slides. The slits are each 1.3 arcsec wide by 15 arcsec long, spaced on 19.6 arcsec (4 mm) centers. This remotely configurable unit is significantly more complicated than the usual method of mounting punched or etched slit-masks in the instrument, but is necessitated by the flexibility demanded by the queue-scheduling of the HET. On any given night, a number of multiobject projects may be executed, and management of the instrument setup to allow for all the possibilities is a daunting task. The MOS unit can be configured in less than 5 minutes, allowing scientists to adjust slitlet coordinates up to the time of the observation (if necessary), and allowing small adjustments to be made to the setup, which would be impossible with masks.

2. DESIGN TRADEOFF: MASKS VS. MOS UNIT

When considering the design of a multiobject unit for the HET, an important factor to keep in mind is the small physical size of the HET focal plane, 50 x 40 mm. Similar instruments, such as the VLT and Keck, have focal planes that are 200-300 mm in size. The small size of the HET focal plane limits our ability to position punched masks very precisely, drive motorized slits from multiple sides, or have adjustable slit widths via moveable jaws. It puts tight constraints on the design of an instrument for doing multiobject spectroscopy on the HET.

2.1 Flexibility and ease of setup

Many existing multiobject spectrographs use object slit masks that are custom fabricated for desired fields. The most popular fabrication methods include external or onboard punching machines, laser cutters, or photochemical etchers. Custom fabrication of masks gives the advantage of tailoring the slits to individual lengths and widths dependent on the object types and distribution in the field, but with this flexibility come some disadvantages. The masks typically have to be made at least a day in advance and a number of them have to be carried onboard the spectrograph for observations during the whole night. This may not be a large problem for telescopes with dedicated observing nights, but for the queue scheduling of the HET, the quantity required for one night becomes limiting. Onboard punch units add some flexibility to when the masks are made or loaded, but the quality of the slits from these units is poorer than from other machines. Registration and rotation adjustment of masks on the field add setup time, which needs to be as short as possible on the HET with typical object track times of approximately 1 hour. A fast and repeatable MOS setup technique is necessary to maximize observing time on target for the HET.

The main drawback of our MOS unit is the loss of flexibility in placing slitlets of varying lengths or widths, or in multiple sets (if only a limited wavelength range is needed). The other alternative for regaining this ability was to use an instrument-mounted slit punch, as in the ESO Multi-Mode Instrument (EMMI)¹⁰, and generate masks in real time. However, analysis of EMMI slit masks revealed that, while the slitlets are of high quality and failures seem relatively rare, the irregularity of the slit jaws (~5%) was larger than desired. This especially appears when multiple adjacent punches are made to increase the slit

length, where a sawtooth pattern can emerge. There are also long term maintenance issues associated with the frequent need to replace the punch heads on such an instrument.

2.2 Quality of slits

The quality of slits becomes extremely important when it comes to flat fielding and sky subtraction for faint objects. Initial tests at McDonald Observatory indicated that very high quality slits could be fabricated by means of vacuum-deposited aluminum via shadow-masking. We have achieved <2% peak-to-peak width variation for the 1.3 arcsec (300 μm) wide slits with this technique. This is better quality than possible with punched masks and surpasses our requirement of 3% rms variations. Slit irregularities at the ~ 5% level, as in EMMI, result in flat fielding residuals that can reach 10% and affect background subtraction.

Laser cut masks can provide very high quality slits. The Canada France Hawaii Telescope (CFHT) Multi-Object Spectrograph / Subarcsecond Imaging Spectrograph (MOS/SIS) uses this technique. The slits from this laser cutter exhibit positional accuracy of $\pm 4 \mu\text{m}$ and slit irregularities of only 2 μm rms.¹¹ Masks are produced from direct images of the field to be observed, which alleviates any problems in matching slit positions to instrument distortions over the field. The disadvantage of this system was the prohibitive cost of the laser cutter. Note that the longslit mask on the LRS was produced by laser cutting.

The Keck Low Resolution Imaging Spectrograph (LRIS) uses punched masks.¹² With this technique comes problems such as the necessity to correct for temperature expansion of the mask when it is installed in the spectrograph on the telescope. Slits that can be positioned in real time before an observation make final adjustments such as this easier to manage. The slits from the punching machine are accurate to 3% in width. The masks can be made in 10 minutes, but cannot be inserted into the spectrograph while it is in the telescope, requiring them to be prepared the previous day.

The ESO VLT FOcal Reducer and low dispersion Spectrograph (FORS) uses moveable jaws for the slitlets.^{13,14} This system is the most like our MOS unit of any discussed here, but the larger focal plane size on the VLT allowed more slits with adjustable widths.

2.3 Number of objects

Although the trend seems to be toward more and more objects per exposure for large surveys, many of the current instruments have the capability of only 10's of objects at a time. Due to the small size of the HET field of view, 4' x 3.5' (50 mm), we fall on the low end at 13 objects. The FORS instrument is very similar in design, but the somewhat larger FOV and much larger physical field size afforded the ability to increase this number up to 19 and to add the capability of variable slit widths using moveable jaws. Table 1 shows a comparison of instrument characteristics for a number of multiobject systems.

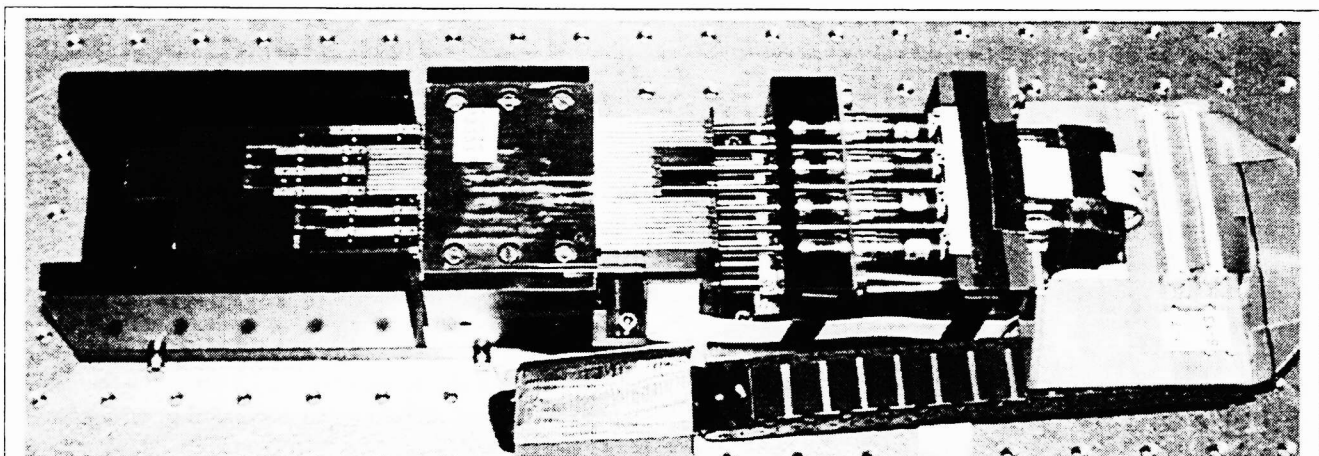


Figure 3. The LRS MOS unit. Stepper motors on the right side attach to lead screws via miniature bellows couplings. The lead screws attach via brass nuts to rails (or slides) that slide through v-groove blocks on cross-roller bearings. The slitlet holders attach to these rails on the left side of the blocks. The slitlets can be seen on the left side of the unit. Every other slit, beginning with the bottom one, has a mask to cover gaps between the slit substrates. The components in the MOS unit and mechanical design are described in detail in the text.

Table 1. Characteristics of multiobject spectrographs.

	PUNCHED MASKS	LASER-CUT MASKS	ONBOARD PUNCH UNIT	MULTI-SLIT UNIT	MULTI-SLIT UNIT
Instrument	Keck LRIS ¹²	CFHT MOS/SIS ¹¹	ESO NTT EMMI ¹⁰	ESO VLT FORS ^{13,14}	HET LRS MOS
Number of objects	40, 80	90	25	19	13
Angular size of field	6' x 8'	10'	5' x 8'	6.8' x 4' or 3.4' x 2'	4' x 3.2'
Physical size of field	265 x 340 mm	83.6 mm	336.6 mm	218 mm	50 x 40 mm
Object density (# objects / arcmin ² of field)	0.83, 1.67	0.9	0.62	0.70	0.81
Number of masks in instrument	10	3	4 blanks / night	---	---
Mask positioning accuracy	0.05"	kinematic		---	---
Slit positioning accuracy	0.07 mm (0.1") over 140 mm	± 4 μm		< 8 μm	0.8 μm
Slit positioning repeatability	---	---	---	< 5 μm	< 1 μm
Slit length	3.9" 2.8 mm	0.14" (min) 0.02 mm (min)	5.3", 8.6" 1, 1.6 mm	22" 12 mm	15" 3.5 mm
Slit width	0.7", 1.4" ~ 1 mm	0.14" (min) 0.02 mm (min)	0.80", 1.02", 1.34", 1.87" 0.15, 0.2, 0.25, 0.35 mm	0.3" (min) 150 μm, ±10 μm acc., 3.5 μm rep.	1.3" 0.3 mm
Slit width variations	3%	2 μm rms	~ 5% 3.3% p-p measured from data	straightness: ± 0.5 μm over 11.5 mm length; roughness: ± 0.2 μm	< 2% p-p
Setup time	100 sec			20 sec	< 5 minutes
Mask manufacturing time	10 minutes	10 min / 50 slits	real time	---	---
Mask configuration limitations	inserted offline		1 punch head per night, use image from EMMI	---	---

3. MOS UNIT DESIGN

The LRS MOS unit is pictured in Figure 3. The HET field of view available to the LRS MOS unit is 4 x 3 arcmin, 4 arcmin in the slit length direction. The unit is very similar in design to the VLT FORS MOS, except for the scale. On the LRS, 4 arcmin corresponds to 50 mm in physical size. In order to fit the maximum number of slits into this area, only miniature components could be used. 13 slitlets of 15 arcsec length and fixed 1.3 arcsec width was chosen as the configuration for the optimal use of available space. FORS, on the other hand, allowed 19 slits with 22 arcsec length and moveable jaws for changing the slit width. The FORS focal plane is 218.4 mm in size, four times larger per side than that of the HET LRS.

The slit length of 15 arcsec was a good compromise between getting enough sky around the object for good sky subtraction and maximizing the number of slits in the field. Our configuration is somewhat limited when compared to what can be done with customized masks. The nominal slit width of 1.3 arcsec was chosen to match the expected typical delivered images from HET once SAMS is installed. The HET site appears to have intrinsic seeing of 0.8-1 arcsec and the HET optics are designed to deliver 1 arcsec images under the best seeing conditions.¹⁵

The CCD on the LRS, 3000 x 1000 chip, is a good format for maximizing the wavelength coverage. We use ~ 750 pixels out of 3000 and cover nominal wavelength ranges of 407-1170 nm (g1) and 426-730 nm (g2) with each grism. This results in a delta wavelength shift of approximately 25% when using the MOS unit.

The smallest cross-roller bearings available from Schneeberger allowed the slits to be placed on 4 mm centers, which gave ~ 20 arcsec slit separation. Cross-roller bearings have lower friction at higher preload than ordinary ball bearings and are highly preferred for this high precision application. Due to severe space constraints around the HET focal plane, the slits could only be driven from one side. Even if space had been available on both sides, the miniature scale of the components would not have allowed sensing for collision avoidance if the slits had been driven from both sides. Even a scale the size of FORS does not allow for a foolproof collision avoidance system.¹⁶

4. DESCRIPTION OF COMPONENTS

4.1 Mechanics

The mechanical design of the MOS unit was driven by the smallest available stepper motors (#36 in Figure 5), which were 10 mm in diameter. Initially we investigated Epson stepper motors used in printers, but in early tests it was discovered that they had insufficient torque for our application. For the final design we selected Model AM1020 stepper motors (manufactured in Germany by F. Faulhaber GmbH and distributed by Micromo in the US) which are 10 mm in diameter by 18 mm long and incorporate a 16:1 gearbox. By staggering the motors and building 2 banks, it was possible to fit them onto 4 mm centers, allowing 13 slitlets over the FOV. This configuration can be seen in Figure 4. The mechanical layout of whole MOS unit is shown in Figure 5.

The rest of the MOS components are custom designed. The cross-roller bearings (#102 in Figure 5) are made by Schneeberger. They manufacture the smallest ones available, which have 1.5 mm rollers. The torque requirements are very tight for this design, so we needed the lowest friction bearings possible.

The design requires that the slitlet substrates (#1 in Figure 5) be extremely parallel to have uniform gaps between them and no contact while moving. The total travel of the slits is 40 mm, of which 36 mm is used in practice to allow for limit sensing at the ends. In order to meet this constraint, custom blocks with v-grooves (#103 and #104 in Figure 5) were all machined simultaneously. The upper block has 13 grooves machined into hardened steel. Each slide (in between #103 and #104 in Figure 5) is separately preloaded from below with springs (#49 in Figure 5) via a set of 13 individual v-groove blocks (#104 in Figure 5) to sandwich the slides. The design is so compact that we also ordered custom components from Schneeberger for the stages, which are designed to exactly fit the slitlet substrates. Total motion of the stages is no more than 40 mm with tight space constraints.

The lead screws (#55 in Figure 5) on the stages (from A. Steinmeyer GmbH) highly over resolve the required slitlet motions. They are custom designed with 0.25 mm pitch stainless steel threads and brass nuts (#81 in Figure 5) to interface to the Schneeberger parts. The resulting motions are 0.8 microns per step. The HET plate scale is 205 microns per arcsec. The lead screws are mounted in preloaded ball bearings and mated to motors with miniature bellows couplings (#59 in Figure 5). In designing such a miniature system, one has to assume very low efficiency of the lead screws to end up with sufficient torque in the final assembly.

The stages cannot be encoded because of the small scale, so we needed a precise home for each one. We chose MyCom G type transistor-based microswitches (#38 in Figure 5), which are accurate to better than 1 micron. These switches are very reliable in practice and were also used on the VLT FORS instrument. The end of travel at the fully extended position is sensed by plastic physical microswitches (#85 in Figure 5). Tests of slitlet homing with an accurate machine gauge block showed better than 1 micron repeatability, as was expected. After many full range motions, the stages repeat to better than 1 micron, when moved individually.

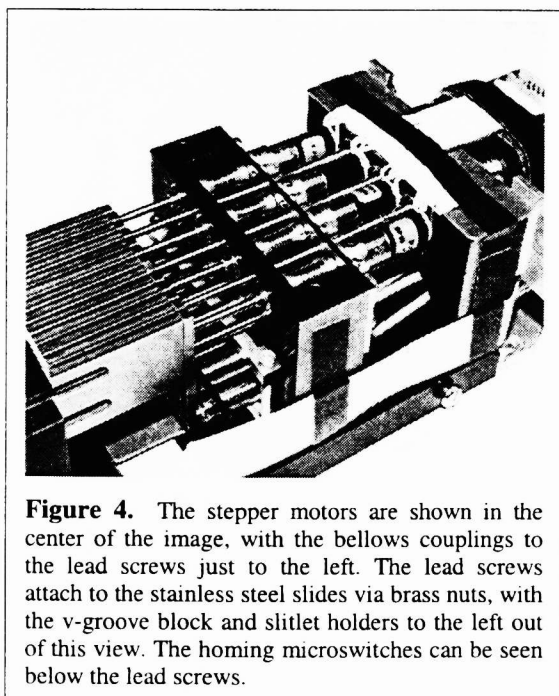


Figure 4. The stepper motors are shown in the center of the image, with the bellows couplings to the lead screws just to the left. The lead screws attach to the stainless steel slides via brass nuts, with the v-groove block and slitlet holders to the left out of this view. The homing microswitches can be seen below the lead screws.

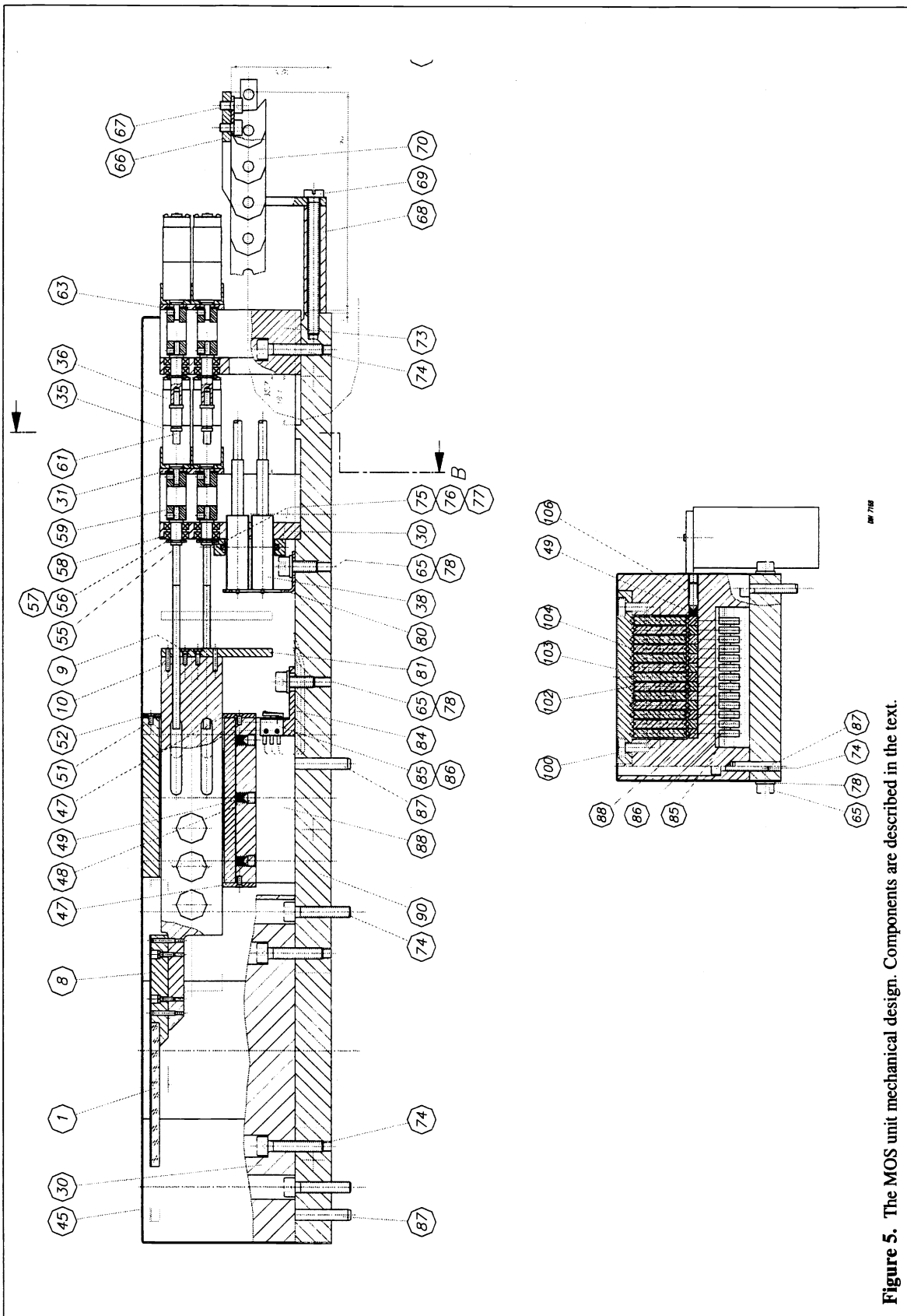


Figure 5. The MOS unit mechanical design. Components are described in the text.

4.2 Electronics

As with the rest of LRS, we chose a simple robust stepper motor driver, the Cyberpak Model HS-20. Each \$400 board provides 4 stepper motor channels and many I/O channels. Up to 16 boards can be used in parallel with the ability to move every motor simultaneously. For the MOS unit we use 4 boards and custom stepper motor drivers based on the Motorola SAA1042 chip. The motors are 2 phase in bipolar mode at 6 V operating voltage. The stepper motor driver electronics are housed in a separate box (shown in Figure 6) mounted on the LRS below the filter wheel. RS-232 communications and power are passed by the main LRS electronics box, a configuration which avoids power supplies lying close to instrument. The MOS unit is driven from the box by a special ribbon cable and connectors that have a dense pinout and are very reliable.

4.3 Optics

Because the MOS slitlets are only driven from one side, the configuration lead us to depositing slits onto optical substrates. We used fused silica substrates, 3 x 3.7 x 52.5 mm in size. Fused silica was chosen for its low coefficient of thermal expansion (CTE) and high strength, along with its optical properties. Because of the "match stick" configuration of substrates, a high strength material that could easily be polished was essential. The substrates were manufactured by High Lonesome Optics, in Ft. Davis, TX. To obtain maximum slit length across the substrate, we specified no edge bevels and no chips on the substrates. The dimensional requirements are 3.7 +0/-0.05 mm on the width and 3 ±0.01 mm on the height, which made them very difficult optical components to make, but they were successfully manufactured.

Following a series of slit manufacturing tests, we decided to fabricate them by vacuum depositing aluminum onto the substrates with a 0.011-inch diameter wire shadow mask. Following inspection, successful slitlets were overcoated with a MgF₂ quarter wave antireflection coating on both sides, which also serves as a protective layer for the aluminum. The resulting precision of the slit width was < 2% peak-to-peak variations. This surpassed our goal of < 3% rms variation in slit width.

The slitlet substrates are bonded to precision invar holders (#8 in Figure 5), designed to interface with the Schneeberger stages. We used Master Bond EP 30 LTE epoxy, which has a low CTE. The substrate and holder were bonded in a jig to insure a straight match. Any tilt to the interface would cause the slitlet substrates to come into contact when moving. The near zero CTE of the fused silica substrate lead us to choose Invar 36™ for the metal interfacing holders to address the concern of small thermal expansions amplifying into movements of the slits. Invar masks (above #1 in Figure 5) are mounted to every other slitlet substrate to cover the gaps and to block scattered light between substrates. The width of masks was chosen such that scattered light would require 2 bounces to get through. The masks were manufactured by Photo Design of Arizona Inc. in Tempe, AZ, by photochemical etching of a 200 micron thick Invar sheet. Various experiments showed that the only useful finish was bluing the Invar to dull the surface. These masks are mounted on the slitlet substrates using Dow Corning brand silicone sealant. This removable adhesive was used initially to test our mask positioning ability and may be replaced with epoxy in the future. The mask was viewed through a binocular magnifier to insure that it aligned properly with the slit underneath. Three dabs of the silicone were used for the bond with short pieces of 300 micron thick wire to set the mask height. The assembly was cured in a fixture. The final finishing step was to use a Testors matte black enamel paint marker to blacken all surfaces except in the immediate vicinity of slits. This approach seems to have been very successful in blocking stray light between the slitlets (see Figure 9). Figure 7 shows the 13 slitlets mounted to their stages in MOS unit.

5. CONTROL AND INTERFACE

5.1 Slitlet configuration

In order to realize the flexibility that the MOS unit offers, it is important to have a straightforward user interface. The unit is controlled via a modified NOAO instrument control environment (ICE) interface, as adopted by McDonald Observatory for telescope and instrument control. Cybervek commands for the Cyberpak controller are embedded in the interface. At the highest level, the MOS unit is configured using a file from disk, which contains offsets of the slits in millimeters from the center of the field. The ICE interface also provides low level commands for moving individual slits during engineering tests. When a multiobject observation comes up in HET queue, the resident astronomer selects the appropriate configuration file

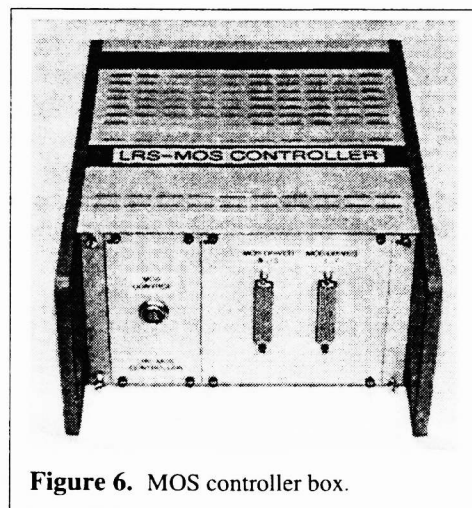


Figure 6. MOS controller box.

and the MOS unit is configured in a few minutes. The setup file is generated by the program Monte, available as a stand-alone program or via a website for registered users. The user inputs a list of object coordinates with priorities and Monte outputs an optimal position angle (PA) and configuration file for the MOS unit, along with wavelength coverages for each object. A detailed description of the Monte algorithm is beyond this paper, but an outline of the setup optimization is given below.

The positioning of slitlets constitutes a particularly difficult optimization task. If all parameters were to be optimized using the same method (e.g. central coordinates, position angle, slitlet positions), the number of parameters would be quite large and the rate of convergence slow. The quality-landscape (the shape of the goodness in the phase-space of the global solution) is very complex: e.g. even a slight shift in the central coordinates can ruin a very good solution. Our technique is to split the optimization task into four parts.

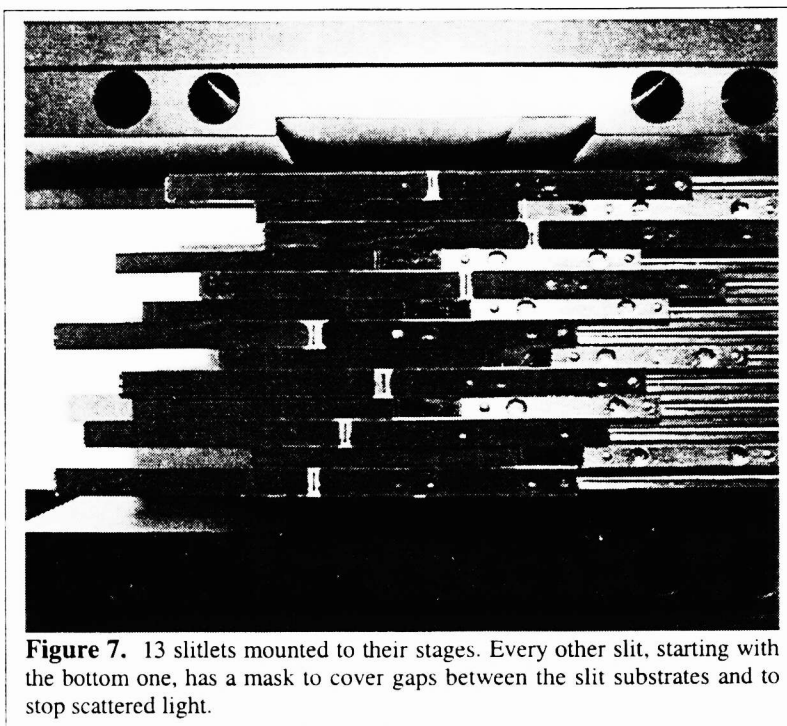


Figure 7. 13 slitlets mounted to their stages. Every other slit, starting with the bottom one, has a mask to cover gaps between the slit substrates and to stop scattered light.

The first part is PA pre-selection. In order to insure that as many slits as possible are used in a solution, the catalogue is first checked for potentially good position angles using a Fourier analysis of the projected object positions for many position angles. This analysis is then used to find a good first guess at the start of the further optimization process. Optimization methods for the other parameters which can use this information (e.g. our Monte Carlo method) benefit considerably from this pre-optimization.

The second part is 1-D optimization. For a given set of fundamental parameters (RA, Dec, PA), the position of the slitlets along the slit direction, Y_{slit} , is obtained by projecting the objects onto the slit and performing a simple cross-correlation with the slitlet mask, using a soft mask in order to keep objects away from the slit edges.

The third part is slitlet assignment. Once Y_{slit} has been determined, the best candidate object available is chosen for each slit. "Best" is determined by the product of the slit position (in order to keep the objects centered) and several optional factors: object priority ($=0$ for highest priority objects which *must* be included, ≥ 1 for normal objects), wavelength coverage (so that the desired spectrum is on the CCD), and relative source brightness (in order to avoid a mixture of bright and faint sources).

The fourth part is global optimization, using one of three methods. Parts 2-3 are repeated for many sets of fundamental parameters (RA, Dec, PA) and optimized using several standard robust optimization techniques.

- 1) The Simplex Algorithm uses *highmoeba*, a maximization routine adapted from the Numerical Recipes minimization routine *amoeba*.¹⁷ The simplex can have a difficult time dealing with the multiple solution peaks, but many independent tries (≥ 10) and somewhat fewer iterations (as low as 100) usually result in quite adequate solutions.
- 2) A Monte Carlo routine can be used for intelligent brute-force searches. This method is our favorite, as it can map out the difficult quality-landscape in a reasonable amount of time (measured in the number of function calls) due to the fact that each optimization samples a line on the sky. Thus, after 1000 iterations, the sampled solution space consists of 1000 lines at semi-random position angles, clustered near the center of the catalogue field. This is much more effective than plowing through a fixed grid and easily avoids the trap of focussing in on secondary maxima. Also, this method can trivially use the information obtained by the PA pre-selection process to avoid PAs which are unlikely to produce adequate solutions.
- 3) A genetic algorithm has been tried via the *evoC* package from the Technische Hochschule Berlin. This algorithm uses 2 populations and 10 children per generation (in *evoC*-jargon, a (1/1,10) optimization). In principle, this may be the best

way to find the absolute optimum parameter set, but in practice, the effort may not be worth the small increase in the number of slitlets per exposure.

The Monte Carlo algorithm is our favorite and is the standard choice for use with the Marcario LRS. The optimization engine is available over the internet (<http://www.uni-sw.gwdg.de/~hessman/Slitlets>) to registered sites and the Monte-Carlo stand-alone program Monte (written in GNU Objective-C) is available to all HET users. A version is also available for the VLT/FORS1 and FORS2 spectrographs, both of which have MOS units.

5.2 Setup on a field

Setup on a multiobject field is no different than setup for a longslit observation, beginning with slit units and grisms out of the beam to image the field. The HET has no natural axis, so setting up at an arbitrary PA is no different than setting up at the parallactic angle, which is the default. The rotation axis of the tracker is precisely encoded and this information is passed to the ICE environment and embedded in data headers. Since no rotation adjustments are necessary for configurable slits, as often is the case with a punched mask, setup is simply a matter of placing one of the objects onto its slit. Following display of the initial acquisition field, the resident astronomer identifies the pixel location of one of the objects and uses an ICE-based utility to offset the telescope the appropriate distance under guider control. Limited experience indicates that it will be possible to setup a multiobject field in about 10 minutes. In the observing sequence, the field image and slit image are saved prior to moving the grism into the beam for the spectroscopic exposure.

6. PERFORMANCE

6.1 Positioning

The precision requirements for the MOS unit, $0.2 \text{ arcsec} = 40 \text{ microns}$, are easily met by the unit. Tests during commissioning showed that when all 13 slits are driven simultaneously, 2 slits do lose steps. This behavior is due to the 4 amp current required to drive them all simultaneously being right on the edge of the supply limit. If slits are driven in groups of a few, they are absolutely repeatable. The control program currently moves the slits individually which is slow, but it will be changed to move them in small groups once we have sufficient data on position repeatability. Before each configuration the unit is homed to give precise positions for each slit and remove any problems associated with losing steps on the previous setup.

A set of tests that offset the slits in 60 pixel increments across the CCD chip was performed during commissioning. From these data we were able to generate an optical distortion map of the LRS and use fits to slit position offsets to correct for it in the MOS configuration files. This method was very successful and resulted in accurate setup files for multiobject fields during commissioning. Limited data on slit positioning repeatability show that it is within 0.24 pixels, or 0.11 arcsec. A second set of tests, which offset the slits by increments of 3 mm, allowed us to relate the optical distortions (measured in pixels) to movements of the slits (measured in mm) on the sky via the plate scale of the LRS.

6.2 Imaging Quality

The slits produce gaussian FWHM profiles of $4.6 \pm 0.15 \text{ pixels}$ over the entire field in imaging mode, corresponding to $1.1 \pm 0.04 \text{ arcsec}$. Dispersed spectra of Ne and HgCdZn comparison lamps show FWHM of spectral elements of 1.21 arcsec, with no more than 0.018 arcsec degradation at the ends of the spectrum. The glass substrates have no effect on the image quality of the LRS, as modeled by Cobos.⁷

6.3 Sky Subtraction

The HET with its silver mirror coatings is designed

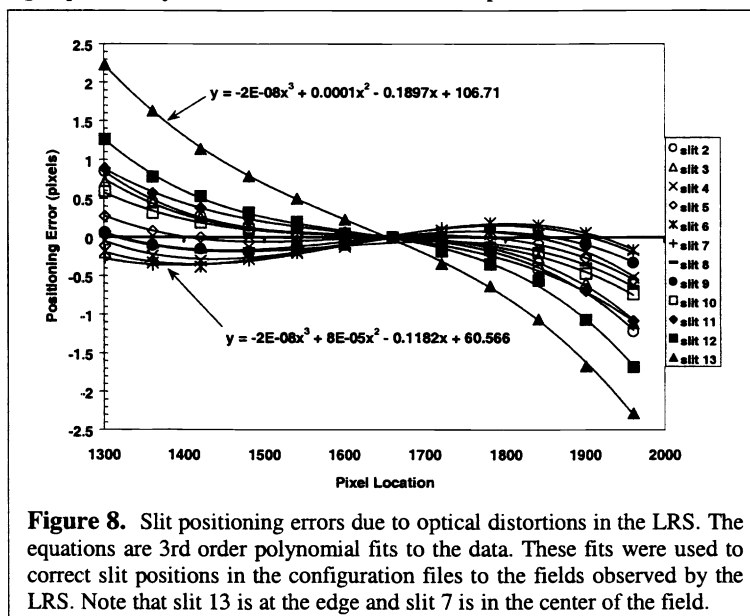


Figure 8. Slit positioning errors due to optical distortions in the LRS. The equations are 3rd order polynomial fits to the data. These fits were used to correct slit positions in the configuration files to the fields observed by the LRS. Note that slit 13 is at the edge and slit 7 is in the center of the field.

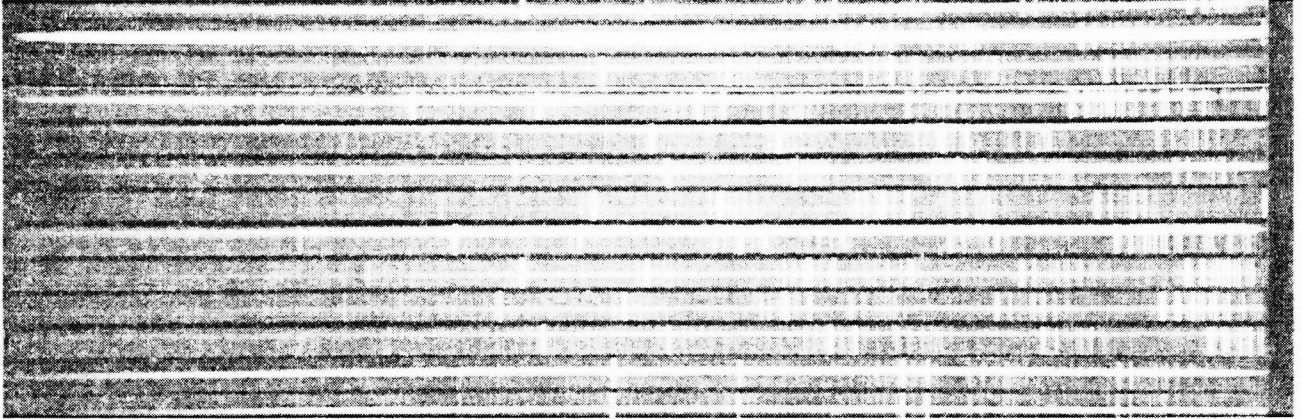


Figure 9. Open cluster NGC 1496, the first observation of 13 simultaneous objects with the LRS MOS. Cosmic rays have been removed, but the sky has not been subtracted. This observation used grism 2 with nominal wavelength coverage of 426-730 nm. Note the excellent baffling between slits except in one case between slits 10 and 11 (slit 1 is at the bottom).

primarily to operate in the visible and NIR, where strong OH sky lines dominate the spectrum. Sky subtraction systematics can dominate signal-to-noise ratios (S/N) in red spectra due to instrument effects such as flexure. Such effects are especially important for the HET since it has varying pupil illumination during its track, which causes the CCD fringe pattern to change with time. It is currently not possible to completely correct the fringe pattern with a flat field. However, a moving baffle mounted in the spherical aberration corrector will be installed in Summer 2000 to fix this problem and to suppress scattered light. This effect currently limits the quality of sky subtraction beyond 700 nm, primarily affecting the low resolution grism (g1). Until this problem is solved, our approach will be to nod the object a small distance along the slit between exposures in a mode similar to that used in IR spectroscopy. Figure 9 shows an image of spectra from the first MOS observation with cosmic rays removed. Figure 10 shows extracted spectra obtained during MOS commissioning of two galaxies that were suspected to be low luminosity members of the Coma cluster. They illustrate the high quality of spectra and good sky subtraction that can be obtained with the LRS MOS. The exposure time for this observation was 30 minutes in 3.0 arcsec seeing with the 1.3 arcsec MOS slits. Neither galaxy turned out to be a Coma cluster member.

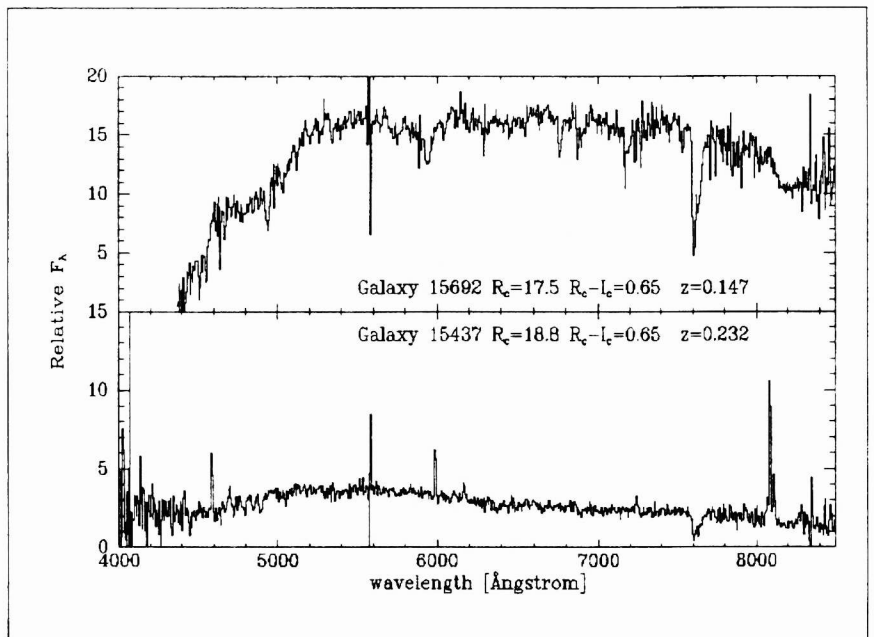


Figure 10. Data from the MOS unit obtained during commissioning. The MOS was set up on 13 objects in a field within the Coma cluster, with the aim of observing faint galaxies that may be low luminosity members of the cluster. Both of these galaxies are more distant than Coma, but these data illustrate the quality of spectra that can be obtained with the LRS MOS. The exposure time was 30 min in 3.0 arcsec seeing (the MOS slits are 1.3 arcsec). Figure by I. Jørgensen.

7. SUMMARY

After one commissioning run, the LRS MOS unit seems to meet all of its design specifications. High quality data with good sky subtraction can be obtained. The throughput of the slits will be matched to the HET image quality when it reaches

optimal operation with the primary mirror segment alignment maintenance system in the spring of 2001. In the HET's current state slit losses can be significant, but high quality data can still be obtained.

The MOS unit on the LRS will enter limited use for partner institutions beginning in May 2000, and will be fully available in the fall of 2000. We are also anticipating its use with a near infrared extension to the LRS, the LRS-J, beginning in 2001.¹⁸ This instrument is quite exciting in that it will provide sky-limited multiobject spectroscopy through the J-band on a 9-meter telescope.

ACKNOWLEDGEMENTS

Mike Marcario of High Lonesome Optics in Fort Davis, Texas, manufactured the MOS slitlet substrates, among other LRS components, but tragically died before the project was completed.

REFERENCES

- ¹ Ramsey L.W., Adams M.T., Barnes T.G., Booth J.A., Cornell M.E., Fowler J.R., Gaffney N.I., Glaspey J.W., Good J., Kelton P.W., Krabbendam V.L., Long L., Ray F.B., Ricklefs R.L., Sage J., Sebring T.A., Spiesman W.J., Steiner M., "The early performance and present status of the Hobby-Eberly telescope," SPIE **3352**, Kona, March 1998.
- ² Gaffney N.I., Cornell M.E., "Scheduling and executing phase II observing scripts on the Hobby-Eberly telescope," SPIE **3349**, Kona, March 1998.
- ³ Barnes T.G., Adams M.T., Booth J.A., Cornell M.E., Gaffney N.I., Fowler J.R., Hill G.J., Nance C.E., Piche F., Ramsey L.W., Ricklefs R.L., Spiesman W.J., Worthington T., "Commissioning experience with the 9.2-m Hobby-Eberly telescope," SPIE **4004**, Munich, March 2000.
- ⁴ Hill G.J., "Hobby-Eberly telescope: instrumentation and current performance," SPIE **4008**, Munich, March 2000.
- ⁵ Booth J.A., Ray F.B., Porter D.S., "Development of a star tracker for the Hobby-Eberly telescope." SPIE **3351**, Kona, March 1998.
- ⁶ Booth J.A., Adams M.T., Ames G.H., Fowler J.R., Montgomery E.E., Rakoczy J., "Development of the segment alignment maintenance system (SAMS) for the Hobby-Eberly telescope," SPIE **4003**, Munich, March 2000.
- ⁷ Cobos Duenas F.J., Tejada de V. C., Hill G.J., and Perez G. F., "The Hobby-Eberly Telescope Low Resolution Spectrograph: optical design," 1998, SPIE **3355**, 424, Kona, March 1998.
- ⁸ MacQueen P., et al., 2000, in prep.
- ⁹ Wolf M.J., Hill G.J., Mitsch W., Altman W., "The HET Low Resolution Spectrograph Multiobject Spectroscopy Unit," 193rd AAS Meeting, Vol. 30, No. 4., poster paper 10.03, Austin, January 1999.
- ¹⁰ EMMI Multiobject Spectroscopy, <http://www.ls.eso.org/lasilla/Telescopes/NEWNTT/emmi/mos.html>.
- ¹¹ LeFevre O., Crampton D., Felenbok P., Monnet G., "CFHT MOS/SIS spectrograph performance," A&A, **282**, 325-340, 1994.
- ¹² Oke J.B., Cohen J.G., Carr M., Cromer J., Dingizian A., Harris F.H., Labrecque S., Lucinio R., Schaal W., Epps H., Miller J., "The Keck Low-Resolution Imaging Spectrometer," PASP **107**, 375, 1995.
- ¹³ Mitsch W., Rupprecht G., Seifert W., Nicklas H., Kiesewetter S., "Versatile multi object spectroscopy with FORS at the ESO Very Large Telescope," *Instrumentation in Astronomy VIII*, SPIE **2198**, 317, 1994.
- ¹⁴ <http://bigbang.usm.uni-muenchen.de:8002/DOCU/tokyo94/tokyo.html>.
- ¹⁵ Hill G.J., "The Hobby-Eberly telescope: instrumentation and current performance," SPIE **4008**, Munich, March 2000.
- ¹⁶ Nicklas H., ***xxx Germany***, private communication.
- ¹⁷ Press W.H., Teukolsky S.A., Vetterling W.T., Flannery B.P. 1992, "Numerical Recipes in C: the art of scientific computing" (Cambridge Univ. Press)
- ¹⁸ Tufts J.R., Wolf M.J., Hill G.J., "Hobby-Eberly telescope low resolution spectrograph J-band camera," SPIE **4008**, Munich, March 2000.